Jinzhe Gong, Martin Lambert, Aaron Zecchin, Angus Simpson, Nicole Arbon and Young-il Kim

Field study on non-invasive and non-destructive condition assessment for asbestos cement pipelines by time-domain fluid transient analysis

Structural Health Monitoring, 2016; 15(1):113-124

Published version available via DOI: http://dx.doi.org/10.1177/1475921715624505

Field study on non-invasive and non-destructive condition assessment for asbestos cement pipelines by time-domain fluid transient analysis

Jinzhe Gong[1], Martin Lambert[1], Aaron Zecchin[1], Angus Simpson[1], Nicole Arbon[1], Young-il Kim[1]

[1]School of Civil, Environmental and Mining Engineering, the University of Adelaide, Adelaide, SA 5005, Australia

Corresponding author:

Jinzhe Gong, School of Civil, Environmental and Mining Engineering, the University of Adelaide, Adelaide, SA 5005, Australia

Email: jinzhe.gong@adelaide.edu.au

Abstract

Asbestos cement (AC) pipelines constitute a significant portion of the potable and waste water systems in many countries in the world, including Australia. Most of the AC pipes in developed countries were installed before 1980, and many utilities are observing that the breakage rate is increasing with the ageing of the pipe. Condition assessment for AC pipes is of important necessity for prioritising rehabilitation and preventing catastrophic pipe failure, however, few techniques are available for direct assessment of the condition of AC pipes and most of them are localised and destructive. This paper outlines a pilot field study of the non-invasive and non-destructive condition assessment of AC pipelines using fluid transient pressure waves. Fluid transient analysis previously conducted by the authors for metallic pipelines is further

developed and adapted to AC pipes for the detection of localised defects. A new sub-sectional condition assessment technique is proposed for determining the effective wall thicknesses of AC sub-sections within a section of pipe bounded by two measurement points. A field trial is conducted in Australia on an AC water main (which has class changes with varying wall thicknesses) to verify the proposed techniques. The wave speeds, lengths and wall thicknesses of sub-sections in different classes are determined and the results are consistent with the information in the design drawings provided by the water utility. This field study, for the first time, verifies that controlled fluid transient waves can be used as a tool for non-invasive and non-destructive condition assessment of AC pipelines.

Keywords

asbestos cement pipeline, condition assessment, hydraulic transient, water transmission and distribution system, water hammer

Introduction

Asbestos cement (AC) pipelines were introduced in the 1920s and extensively used for water distribution systems (WDS) from 1950s to 1970s in Australia, Europe and North America. Although the installation of new AC pipes was largely curtailed in the 1980s due to health concerns, the remaining AC pipes still form a significant portion of the WDS in many cities. It is estimated that AC pipes account for 12 to 15% of WDS in North America, where the number is much higher in some regions[1].

AC pipes are known to deteriorate mainly by three processes: lime leaching[2], sulphate attack[3] and biodegradation[4, 5]. Free lime (calcium hydroxide) leaches into the water conveyed by, or surrounding, an AC pipe over time through diffusion, resulting in decomposition of hydrated silicates, an increase in porosity and a loss of material strength[2, 6], although typically no apparent reduction in wall thickness is observed. Soft water with a low ion content, such as pure distilled water, can cause lime leaching and wall

deterioration, while acidity can enhance the process[2]. Sulphates in the water and soil surrounding an AC pipe can react with calcium hydroxide to form calcium sulphate, which in turn can react with hydrated calcium aluminate to form calcium sulphoaluminate[3]. The products of these reactions can induce expansion and destruction of the cementitious matrix of an AC pipe[3]. Recent research showed that biofilms that grow on the surface of AC pipe wall can also contribute to deterioration. Wang and Cullimore[4] found a series of bacteria, which can be categorised as heterotrophic bacteria, slime-forming bacteria and acid producing bacteria, in the patina layer on the inner wall of a broken AC pipe that had been in service for 35 years. A further study by Wang et al.[5] showed that these groups of bacteria can make an anaerobic and acidic local environment, accelerating the leaching of free lime and Ca-bearing minerals in hydrated cement matrix, and resulting in the reduction in the effective wall thickness (the part of wall that maintains material strength) of an AC pipe.

With the ageing of existing AC pipe assets and increasing public demand for accountability, many water utilities need better strategies to manage their AC systems, for which the understanding of the present condition of their AC pipes and the ability to forecast future failure are essential[1]. However, due to the unique material properties and deterioration mechanisms of AC pipes, the number of techniques available for assessing their condition is limited compared to those available for ferrous pipes. Environmental assessment techniques[7], such as water quality testing and soil testing, are useful for assessing the possibility of deterioration but are indirect and cannot yield information as to the actual present condition of a pipeline. Selective sampling test techniques, such as mechanical testing[6], phenolphthalein testing[8], hardness testing[9, 10] and scanning electron microscopy with energy dispersive X-ray (SEM/EDX) analysis[11], require the removal of short sections, or coupons, from an AC pipe, which is a destructive and expensive process. In addition, results from selective sampling tests can sometimes be misleading since the deterioration of a pipeline is typically non-uniform. It is also worth noting that destructive testing of AC pipes should be avoid if possible to prevent the release of asbestos dusts because they are extremely harmful to the health.

For non-destructive direct inspection of the wall condition of AC pipes, currently there are two technologies available: georadar-based wall thickness measurement[12] and acoustic-based average wall thickness estimation[13]. The georadar technique can realise high-resolution in-line inspection for AC mains greater than 200 mm, but the cost is high and access to the interior of the main is required[14]. The acoustic average wall thickness estimation technique is non-invasive and non-destructive, but it is a low resolution technique because only the average wall thickness between two measurement points can be determined. The determined average wall thickness can be misleading if the tested pipe section has unregistered pipe replacements, material changes or class changes. A more efficient and accurate non-invasive and non-destructive AC pipe condition assessment technique is needed.

Research in the past two decades has shown that fluid transient waves, also known as water hammer[15], can be used for pipeline leak detection[16-21], blockage detection[22-26] and, more recently, condition assessment[27-30]. A controlled pressure wave can be generated by abruptly closing a side-discharge valve. The incident wave propagates along a pressurised pipeline and reflections occur when the wave encounters any physical changes, such as a reduction in wall thickness. The wave reflection propagates towards the source of the incident wave (the side-discharge valve) and can be measured by pressure transducers. The measured pressure traces are then analysed in either the time or the frequency domain[25, 31] to determine the location and severity of the defects. Although a number of transient-based pipeline fault detection or condition assessment techniques are reported in the literature, field verifications are scarce so far. Meanwhile, the focus of previous research in this area has mainly been on metallic pipelines, though plastic pipes are drawing more attention recently[32-34]. To the knowledge of the authors, except the preliminary pressure testing studies of Stephens[35], no studies on transient-based AC pipe fault detection or condition assessment are reported in the literature. Investigations, especially experimental studies, on transient-based condition assessment of AC pipes are needed because the material properties and deterioration mechanisms of AC pipes are different from metallic and plastic pipelines.

The research reported in this paper is a pilot field study on condition assessment of AC pipelines using fluid transient waves. Techniques proposed by the authors for fault detection in metallic pipelines[29, 30] are further developed and adapted to AC pipes to detect localised defects (e.g. localised wall deterioration, air pockets). A sub-sectional condition assessment technique is proposed to achieve efficient condition assessment for the whole pipe section tested with medium resolution. A section of pipe bounded by two measurement points is divided into several sub-sections for analysis. The sub-sectional condition assessment gives the average wave speed, length and wall condition of each of the sub-sections. Field data measured from an AC water main with known class changes (varying wall thicknesses) are used to verify the feasibility of transient-based condition assessment for AC pipes. The wave speeds, lengths and effective wall thicknesses for the sub-sections in different pipe classes are determined, and the results are found to be consistent with the information in the design drawings provided by the water utility. The procedure for detecting localised defects in AC pipelines is also discussed using the analysis on a specific wave reflection as an example. Since similar wave reflections can be induced by various types of localised defects, techniques for determining the most likely type and properties of a defect are highlighted. This research, for the first time, verifies that controlled fluid transient waves can be used as a tool for non-invasive and non-destructive condition assessment of AC pipelines.

Theory and basic equations

The speed for a fluid transient pressure wave travel in a pressurised elastic pipeline is given by one dimensional water hammer theory[36, 37] by the following relationship

$$a = \sqrt{\frac{K/\rho}{1+(K/E)(D/e)c}} \tag{1}$$

109 in which a is the wave speed, K is the bulk modulus of elasticity of fluid, ρ is the density of fluid, E
110 is Young's modulus of the pipe wall material, D is the pipe internal diameter, e is the wall thickness and
111 c is a factor depending on the restraint condition of the pipeline[37].

112 Wave reflections are induced when an incident pressure wave encounters any physical changes in a pipeline,
113 such as a pipe section with a deteriorated wall. Gong et al.[29, 38] analysed the pressure wave reflection and
114 transmission in a copper pipeline induced by a thinner-walled section. In that work, it was shown that the
115 size of a pressure wave reflection induced by a deteriorated pipe section is related to the size of the incident
116 wave and the degree of change in pipeline impedance. To remove the dependence on the incident wave, the
117 wave reflection can be normalised by dividing itself by the size of the incident wave, and written as

$$H_r^* = \frac{\Delta H_r}{\Delta H_i} \tag{2}$$

118 where H_r^* is the dimensionless head perturbation of the reflected wave, ΔH_r is the dimensional reflected
119 head perturbation, which is negative if the head induced by reflection is lower than that of the incident wave;
120 ΔH_i is the dimensional head perturbation induced by the incident pressure wave, which is positive if it is
121 generated by an abrupt closure of a side-discharge valve. The value of H_r^* is governed by[29]

$$H_r^* = \frac{B_r - 1}{B_r + 1} \tag{3}$$

122 where B_r is the ratio of the impedance of the deteriorated pipe section to that of an intact section, and
123 pipeline impedance is defined as

$$B = \frac{a}{gA} \tag{4}$$

Defect detection for AC pipes using fluid transient wave reflection

For metallic pipes, wall deterioration is typically internal or external wall thinning due to corrosion[28, 30]. For AC pipes, however, wall deterioration is typically a reduction in the effective AC thickness due to loss of Ca-bearing minerals, while the physical thickness of the wall, as if physically measured by a device, is not changed. As a result, an assumption is made that wall deterioration of an AC pipe can be modelled by a reduction in effective wall thickness, i.e. decreasing from the original wall thickness e_0 to the remaining effective wall thickness e_{eff}, either from internal, external or both sides. The relative change in wall thickness is defined as e_{rc} and represented by

$$e_{rc} = \frac{e_{eff} - e_0}{e_0} \tag{5}$$

A reduction in effective wall thickness results in a decrease in wave speed and impedance[29]. Using Eqs. (1) and (5), the wave speed in a deteriorated AC section with an effective wall thickness of e_{eff} can be derived as

$$a_1 = \sqrt{\frac{(K/\rho)(1+e_{rc})a_0^2}{(K/\rho)+e_{rc}a_0^2}} \tag{6}$$

where a_0 is the wave speed for an intact AC pipeline with a wall thickness of e_0. The impedance ratio between a deteriorated AC pipe section and an intact section is the ratio between the wave speeds since the cross-sectional area does not change. As a result, B_r can be written as

$$B_r = \sqrt{\frac{(K/\rho)(1+e_{rc})}{(K/\rho)+e_{rc}a_0^2}} \tag{7}$$

Substituting Eq. (7) into Eq. (3) results in the following expression for the dimensionless reflected head perturbation

$$H_r^* = \frac{\sqrt{(K/\rho)(1+e_{rc})}-\sqrt{(K/\rho)+e_{rc}a_0^2}}{\sqrt{(K/\rho)(1+e_{rc})}+\sqrt{(K/\rho)+e_{rc}a_0^2}} \tag{8}$$

Eq. (8) shows that the dimensionless head perturbation of a wave reflection (H_r^*) induced by a deteriorated AC section is related to the relative change in effective wall thickness (e_{rc}) and the wave speed of an intact section (a_0). Eq. (8) can be used to detect localised defects in AC pipes provided that the incident pressure wave is generated on an AC section with a known wave speed (by either calculation or measurement). The relative change in the effective wall thickness in a deteriorated AC section can be determined from the size of the corresponding wave reflection using Eq. (8), and the location of the deterioration can be calculated from the arrival time of the reflection using time-domain reflectometry. If the pressure measurement point is at the source of the incident wave, the arrival time of a wave reflection (relative to the starting time of the incident wave) is the time for the wave to travel twice the distance between the measurement point and the deterioration.

Challenges and countermeasures to field applications

Challenges, however, exist in field applications. Eq. (8) is not directly applicable if the wave speed a_0 is unknown. Measured pressure traces include many reflections and it is needed to distinguish which are significant and worth analysing. Multiple deteriorated sections may be present and located on either side of

154 a measurement point, which can result complex measurements due to the superposition of the reflected
155 waves traveling upstream and downstream. In addition to localised defects, the general condition of the
156 whole pipeline tested is usually of significant interest for water utilities.

157 Techniques are developed to tackle the challenges in the field. Before dealing with the measured data,
158 theoretical analysis on the wave speed and the size of reflection with respect to varying degree of wall
159 deterioration is conducted. The basic equations [Eqs. (1) to (4)] are generally applicable, and Eq. (3) is a
160 general description about how the size of a wave reflection is related to a change in impedance. The effects
161 of friction can usually be neglected within large diameter transmission mains when the flow is small and
162 the length of analysis is within a couple of kilometres[28]. A sensitivity analysis previously conducted by the
163 authors showed that the head reduction in a transmitted wave is usually negligible (less than 1 % after
164 passing through a deteriorated section with wall thickness reduction up to 35 %)[38], so that it can be assumed
165 that the head of a pressure wave is unchanged after passing through multiple deteriorated sections, provided
166 the number of sections is not significant. The theoretical analysis help to set a threshold that can be used to
167 determine which reflection is significant and need further analysis.

168 A comparison of the pressure traces measured at multiple points within the same test can be used to
169 determine the directional information of the source of reflection[30]. A wave reflection arrives at two
170 measurement points in different locations in sequence and with a certain time delay. This time delay can be
171 determined by cross-correlation analysis between the wave front signals as measured by the two transducers.
172 Manually forward or backward time-shifting of one measured pressure trace according to the specific time
173 delay and then plotting it with the other measured pressure trace in the same diagram will make the
174 reflections sourced from either the upstream or downstream of the two transducers line-up. For example,
175 pressure transducer T2 is located downstream from transducer T1 and the time for a wave to travel between
176 them is Δt. Once the pressure responses have been measured by the two transducers, the pressure trace

measured by T2 is shifted forward (delay) in time by Δt and then plotted together with the original trace measured by T1 in the same diagram. The result is that pressure reflections sourced from downstream of T2 as measured by the two transducers will line up in the time axis. Similarly, shifting the original measurement by T2 backward in time and plotting the time-shifted trace with the one measured by T1 will line up reflections from the upstream side of T1.

A *sub-sectional condition analysis* technique is proposed to achieve efficient assessment of the general condition of the pipe section tested. A section of pipe between two measurement points is divided into several sub-sections for analysis according to the sizes and characteristics of the wave reflections. The wave speed, length and wall condition of each sub-section can be determined.

The flowchart in Figure 1 illustrates the proposed procedure of data analysis. Details about how to implement these techniques are illustrated in the following section through a field case study.

Field case study

A field case study has been conducted to assess the feasibility of fluid transient-based condition assessment for AC pipelines. The section of AC pipe involved in the field study has known class changes. The aims of the study include locating the class changes from measured transient pressure traces, the determination of the effective wall thicknesses for pipe sub-sections with different classes using the sub-sectional condition analysis technique, and the detection of any significant localised defects through the analysis of significant transient pressure wave reflections.

Pipeline information

The field work was undertaken in Victoria, Australia in April 2014 on a regional AC transmission main with a nominal diameter (DN) of 300 mm. The total length of the AC transmission main is 7.6 km. It was

198 constructed in the 1960s and buried under ground. The upstream end of the AC pipe was connected to a
199 ductile iron pipe, which was then connected to a water storage tank far upstream. The downstream end of
200 the AC pipe was closed during the test. Major off-takes were also closed during the test. The layout of the
201 section of interest (2.4 km) is given in Figure 2. This AC pipe consists of Class B and Class C DN300 AC
202 sections according to the design drawings provided by the Victorian water utility (Eastern Gippsland Water).
203 The frequent change in pipe class was to encounter the elevation changes along the pipeline. The chainage
204 information from the drawings for the class changes and the location of connection points for the transient
205 test are also shown in Figure 2.

206 The physical properties of the DN300 AC pipe are summarised in Table 1. The dimensions of the AC pipe
207 are taken from Australian Standard 1711-1975 for asbestos cement pressure pipes[39]. The modulus of
208 elasticity of intact AC is 32 GPa as experimentally determined by Beuken et al.[14] from AC pipe samples.
209 The Poisson's ratio of AC is assumed to be 0.2. The ratio of internal diameter to wall thickness is
210 approximately 17.3 for the Class B and 11.6 for the Class C pipe. As a result, the constraint factor c as
211 used in the wave speed formula Eq. (1) is calculated for thick-walled pipe with constraint against
212 longitudinal movement[37]. The theoretical wave speeds for intact Class B and Class C sections are calculated
213 using Eq. (1).

214 *Testing procedure*

215 The testing procedure consisted of the generation of an incident step pressure wave and the measurement
216 of the pressure responses of the pipeline. The three connection points (P23, PB and P28) were either fire
217 hydrants or air valves, which provided access to the main pipe without excavation. A customised side-
218 discharge valve-based transient pressure generator was installed at P23 for the main testing used for the
219 sub-sectional analysis, and shifted to PB and P28 for the more detailed defect analysis. The side-discharge
220 valve was open for several minutes until the pressure in the main pipe was relatively steady. Then the side-

discharge valve was closed abruptly (within 10 ms) to generate a step pressure wave. A pressure transducer was installed at each of the three points to measure the pressure trace during the test at a sampling frequency of 2 kHz. The pressure transducers used are Druck PDCR 810 high integrity silicon flush mounted diaphragm transducers. The pressure range is 35 bar for the measurement stations and 60 bar for the generation site. The natural frequency is more than 28 kHz, the rise time is 5×10^{-6} s and the measurement uncertainty is rated at 0.1% of the full measurement span. The equipment used in the test was the same as that used in a previous field study on a mild steel cement mortar lined (MSCL) pipeline as reported in Stephens et al. [28].

Theoretical analysis on wave speed and size of reflection

The wave speed is of particular interest for AC pipes since wall deterioration typically alters the wave speed but does not change the cross-sectional area. A change in the effective AC wall thickness (due to wall deterioration or class change) will induce a change in the wave speed according to Eq. (1). The theoretical wave speeds for AC pipe sections with different degrees of wall deterioration (i.e. varying effective AC wall thicknesses) are determined to facilitate the condition assessment, and the results are given in Figure 3.

Given a measured wave reflection, the impedance ratio B_r can be determined from the dimensionless head perturbation H_r^* using Eq. (3), and then the wave speed ratio can be calculated. For this particular field case study, however, there are known class changes with varying cross-sectional areas. As a result, changes in the cross-sectional area have to be considered when analysing the reflections induced by pipe class changes. Mathematical manipulation of Eq. (3) to incorporate the impedance terms from (4) into the impedance ratio B_r yields

$$a_r = A_r \frac{1+H_r^*}{1-H_r^*} \tag{9}$$

where a_r is the ratio of wave speeds (the wave speed of the section receiving the incident pressure wave to that of the section from which the wave departs), and A_r is the corresponding ratio of cross-sectional areas. If there is no change in cross-sectional area, e.g. the pipeline under test is uniform in class, then the value of A_r is unity. For this case study, and considering wave propagating from a Class B section to a Class C section, the value of A_r is calculated as 0.969 using the diameter information given in Table 1.

Analysis is also conducted to determine the theoretical size of dimensionless head perturbation induced by varying degree of relative wall thickness changes. Using Eq. (8) and the pipeline information given in Table 1, the variation in the dimensionless head perturbation (H_r^*) according to various relative change in wall thickness (e_{rc}) is calculated for both Class B and Class C AC pipes, and the results are given in Figure 4.

It can be seen from Figure 4 that an approximate 20% reduction in effective AC wall thickness ($e_{rc} = -0.2$, 3.46 mm for Class B and 5.08 mm for Class C) will introduce a negative wave reflection with a size 3% of the incident wave ($H_r^* = -0.03$). This can be used as a threshold to determine the significance of the reflections.

Time-shifted pressure traces

For the main test, an incident step pressure wave (magnitude 8.06 m) was generated at P23. The incident step wave was captured by the transducer at P23 directly after the generation. Cross-correlation analysis showed that it took 1.3355 s and 1.0255 s for the wave front to travel to PB and P28, respectively. Note that for a sampling rate of 2 kHz, the highest temporal resolution is 0.0005 s. The time-shifted dimensionless

head perturbations [H_r^* in Eq. (2)] measured at the three points are given in Figure 5. The start time of the wave front measured at P23 is set to zero. The pressure trace measured at P28 (which is located downstream of P23) is shifted backward in time by 1.0255 s. The pressure trace measured at PB (which is located upstream of P23) is shifted forward in time by 1.3355 s. The time-shifting is undertaken to help to identify the reflections induced by anomalies in the pipe section between PB and P23. Reflections induced by anomalies on the upstream side of P23 (the direction towards PB) as measured by different transducers will line up in time in the time-shifted plot, while reflections from the downstream side of P23 will not. The time shifting was also used by the authors in a previous field study on a MSCL pipeline[30].

The corresponding numerical results of H_r^* for P23 and P28 as calculated by method of characteristics using the theoretical pipe properties and the change in pipe classes shown in the design drawings are also shown in Figure 5. It can be seen that some major reflections (pressure jumps and drops) as measured in the field test are consistent with the numerical results in timing and pattern, which confirms that those reflections were from pipe class changes. There are also discrepancies between the measured traces and the numerical results. It should be noted that the measured pressure traces better represent the pipeline condition than the numerical results do. The real pipeline system is likely to be different from the numerical pipeline model as read from the design drawings because of pipe deterioration and the deviation between the construction and the design. As a result, the data analysis as presented in the following sub-sections is independent of the numerical pressure traces.

The beginning of the pressure trace (0.2 s) measured at the generation point (P23) is contaminated by high frequency pressure oscillations occurring in the stand pipe that connects the side-discharge valve and the main pipe[28]. As clear in the traces, this induced noise at the generator does not have a significant effect on the pressure traces measured away from the generation points (e.g. the dashed line measured at P28).

From the time-shifted pressure traces (Figure 5), five sub-sections (S1 to S5) for sub-sectional analysis are identified based on the lined up reflections that indicate significant and extended change in pressure. Six significant reflections (R1 to R6), which are significant in magnitude (size greeter than 0.03) but short in duration, are also identified for localised defect detection. Details of the analysis are reported in the following sections.

Sub-sectional condition assessment

Sub-sectional condition assessment is implemented on the section between PB and P23 in this paper. The first step is to identify which reflections are induced by anomalies located within the section of interest. It can be seen from Figure 5 that, between the wave fronts measured by P23 (solid line) and P28 (dotted line), reflections at t_1 to t_4 and reflection R5 as measured by P23 and PB (dashed line) are aligned at the same time point. The alignment indicates that the sources of the reflections (the anomalies) are located upstream of P23 (the direction towards PB). In particular, they are located between P23 and PB, with the reflection from an anomaly closer to P23 arriving earlier in time. There are also reflections that do not line up (e.g. reflections R1 to R4 and R6), and they are induced by anomalies located on the downstream side of P23 (the direction towards P28).

The second step is to divide the section of pipe bounded by the two measurement points PB and P23 into sub-sections. Considering the timing and sizes of the aligned reflections (reflections at t_1 to t_4 and reflection R5), the section of pipe between PB and P23 is divided into five sub-sections, as represented by S1 to S5 in Figure 5. The key criterion of segmentation is to check if the aligned reflection introduces a significant pressure change that extends for a period of time (typically more than 0.1 second). Reflection R5 is significant but is too short for sub-sectional analysis. It will be addressed in the localised defect detection. The assignment of sub-sections actually follows the change in pipe class, which will become

clear in the final results. The arrival time of the reflections induced by the boundaries between subsections are denoted as t_1 to t_5 and given in Figure 5. Note that the time t_5 is the time-shifted starting time of the wave front recoded at PB. Considering that the starting time of the wave front measured at P23 has been set to zero and the pressure trace for PB is shifted forward in time to double the original time interval between the wave fronts, t_5 is the time interval needed for a pressure wave traveling twice the distance between P23 and PB.

The third step is to determine the average wave speed of each sub-section, denoted by a_{S1} to a_{S5} for sub-sections S1 to S5. All the sub-sections may already be in a deteriorated state at the time of testing, so that all the sub-sectional wave speeds are unknown and yet to be determined. From the dimensionless head perturbation and Eq. (9), the relationship between the wave speeds of two adjacent sub-sections can be determined. For example, from Figure 5, when a step incident pressure wave travels from S1 to S2, at time t_1, the size of the dimensionless head perturbation (H_r^*) of the reflection is approximately 0.064 (where the magnitude of a head change was determined by fitting a flat line to the pressure trace before and after the head change). As a result, the ratio of a_{S2} to a_{S1}, denoted as a_{r2}, is calculated as 1.102 using Eq. (9) (note that A_r = 0.969 was used in the calculation of a_{r2}). Similarly, the ratios of a_{S3}, a_{S4} and a_{S5} to a_{S1} are calculated as a_{r3} = 1.006 (with H_r^* = 0.003, A_r = 1), a_{r4} = 1.092 (with H_r^* = 0.059, A_r = 0.969) and a_{r5} = 0.994 (with H_r^* = −0.003, A_r = 1), respectively. Note that the dimensionless size of reflection R1 (0.052) has to be subtracted from the readings from the solid line (P23) in Figure 5 to yield the correct values of dimensionless head perturbations for S3, S4 and S5.

For the i th sub-section, the relationship between the sub-sectional wave speed and the sub-sectional length is governed by

$$a_{Si}(t_i - t_{i-1}) = 2L_i \tag{10}$$

where L_i is the length of the i th sub-section. Summarizing the corresponding equations for all the sub-sections, and using the wave speed ratios and the baseline wave speed a_{S1} to represent the sub-sectional wave speeds, the final equation is

$$a_{S1}\sum_{i=1}^{N} a_{ri}(t_i - t_{i-1}) = 2L \tag{11}$$

where N is the total number of sub-sections (5 in this study), a_{r1} is always unity, t_0 is the starting time of the wave front measured at the generation point in the time-shifted dimensionless head perturbation plot (zero in this study), and L is the length of the section between two measurement points (1345 m in this study). The values of t_1 to t_5 and a_{r2} to a_{r5} are then substituted into Eq. (11) to calculate the value of a_{S1}, which is determined as 976 m/s. Using the ratios a_{r2} to a_{r5}, the values of a_{S2} to a_{S5} can be determined and the results are summarised in Table 2.

The fourth step is to calculate the length of each sub-section. This can be achieved by using the previously determined average sub-sectional wave speeds (a_{S1} to a_{S5}) and Eq. (10). The results of the sub-sectional lengths are also summarised in Table 2.

The final step is to determine the remaining average effective AC wall thickness. The effective AC wall thickness of a sub-section is linked to the determined sub-sectional wave speed by Eq. (1). Figure 3 can serve as a look-up chart to obtain the effective wall thickness of each sub-section. The results of the effective AC wall thicknesses for the five sub-sections are also summarised in Table 2.

Comparing the determined sub-sectional wave speeds, sub-sectional lengths and effective AC wall thicknesses with the known class changes (Figure 2), it is apparent that the five sub-sections correspond to the pipe sub-sections with class changes between points PB and P23. The theoretical wave speed and wall thickness for each sub-section when it is intact (as shown in Table 1), and the sub-sectional lengths read from the design drawings, are also presented in Table 2 for comparison. Note that the theoretical results do not necessary represent the 'real condition' of the pipeline since the pipe has been in use for decades and deterioration is expected. The difference in the wall thicknesses between Class B and Class C DN300 AC pipe sub-sections is 8 mm when they are intact or with the same degree of wall deterioration. This wall thickness change is successfully detected with reasonable accuracy. The determined length of each sub-section is also consistent with the designed lengths, where the relative difference is less than 4% in all cases. The results show that all these AC sub-sections have a mild wall deterioration with a reduction in average effective AC wall thickness of up to 2.3 mm. Overall, the results verify that the sub-sectional condition analysis technique is effective for assessing the general wall condition of sub-sections within a long section of pipe bounded by two measurement points.

Detection of localised defects

The previous sub-sectional condition assessment gives the average wall condition of the sub-sections within a long pipe section bounded by two measurement points, which is a medium resolution assessment technique when compared with the low resolution acoustic-based average wall thickness estimation[13, 14]. For significant deterioration with a short length, which are categorised as localised defects in this paper, a different approach, namely localised defect detection, is used for comprehensive analysis of the wave reflection and other known information. The localised defect detection complements the sub-sectional condition assessment by providing high resolution information at specific locations.

Using the threshold of $H_r^* = -0.03$ (representing 20%, or 4 to 5 mm, reduction in the effective AC wall thickness) as discussed in a previous section, six significant localised reflections R1 to R6 are identified in the time-shifted pressure traces in Figure 5. Among the six reflections, only R5 is an aligned reflection. This indicates that R5 is induced by an anomaly located between P23 and PB, and in particular, within sub-section S5, while the other five are from anomalies located downstream of P23 and thus out of the section of interest. The analysis of reflection R5 is shown here to illustrate the process of localised defect detection and how to determine the type and properties of the defect among various possibilities.

Reflection R5 is a significant negative reflection with a short duration. Based on experience and the system information available, the corresponding anomaly is most likely to be: a deteriorated section with a short length, a short section replaced by plastic pipe, or an air pocket. Considering the distance between the anomaly and the generation point is relatively long (over 1 km), the set of test as shown in Figure 5 is not ideal for detailed analysis of reflection R5, as explained in the following. The incident pressure wave generated by the side-discharge valve-based generator typically has a tilted wave front with a rise time of approximately 10 ms. While traveling along a pipeline, the incident wave experiences signal dispersion, which increases the time span of the wave front. As a result, the spatial resolution (the minimum length of a deteriorated section that can be correctly identified) decreases with distance. Numerical analysis conducted by Gong et al.[29] showed that if the length of a deteriorated section is shorter than $T_r a / 2$ (where T_r is the rise time of the wave front and a is the wave speed in the deteriorated section), the recorded wave reflection induced by the short deterioration is not as significant as it would be if it had a length longer than the threshold. Using the wave speed 900 m/s (corresponds to sections with approximately 12 mm effective AC wall thickness remaining) and a rise time of 10 ms as a guideline for this case study, the length threshold is calculated as approximately 4.5 m.

385 The results from another test with the generation point at PB are used to further analyse the anomaly.
386 Compared with P23, PB is much closer to the anomaly under study, so that the wave front as generated at
387 PB is still sharp when it arrives at the anomaly and can deliver relatively high spatial resolution. The time-
388 shifted (start time set to zero) dimensionless head perturbation measured at PB is given in Figure 6. Note
389 that only the part of the trace that highlights the reflection from the specific anomaly under study is shown,
390 and this reflection is named as R5_B in this test.

391 Analysis starts with calculating the change in impedance and wave speed from the size of the reflection
392 using Eq. (3). From Figure 6, the dimensionless size of the reflection is approximately $H_r^* = -0.227$.
393 Substituting this value into Eq. (3), the impedance ratio between the anomaly and the pipe where the
394 generator was located (Class B) is determined as $B_r = 0.63$. The arrival time (when the pressure starts to
395 drop) of the reflection is $t_a = 0.451$ s. As a result, this anomaly is located approximately 219 m downstream
396 of point PB using the sub-sectional wave speed in S5 (970 m/s).

397 The three possible explanations for the anomaly (deteriorated AC, plastic replacement or air pocket) are
398 checked in sequence. If the anomaly is a deteriorated AC section, the relative change in wall thickness is
399 determined as $e_{rc} = -0.723$ using Eq. (7) or (8). Substituting the determined e_{rc} into Eq. (5) and using the
400 determined average effective AC wall thickness of sub-section S5 (15.8 mm) for e_0, the effective AC wall
401 thickness for the assumed deteriorated AC short section is determined as $e_{eff} = 4.4$ mm, which indicates a
402 reduction of 12.9 mm or 75 % from the original condition. Based on engineering judgement, however, a
403 short AC section with such a thin remaining effective AC wall thickness is unlikely to be the real scenario
404 in the field, because pipe sections with such a degree of wall deterioration would have broken even under
405 normal operational pressure conditions. Note that the estimated effective AC wall thickness 4.4 mm is the
406 average wall thickness of a short pipe section if wall deterioration is the case. Considering that wall

deterioration is typically non-uniform along the circumference, a 75 % average wall reduction means some patches may even have a wall reduction more than 75 %. Patches with such as high degree of deterioration are unlikely to sustain the normal operation condition. As a result, the possibility that this anomaly is a deteriorated AC section is eliminated by the analysis.

Now assess whether this anomaly is a plastic pipe replacement. Field workers from the water utility confirmed that polyvinyl chloride (PVC) pipes with a typical sectional length of 4 m were used to replace original AC sections when necessary (e.g. to fix a pipe burst). The PVC pipe used for replacement would have a similar cross-sectional area with the original AC pipeline, therefore, the wave speed ratio a_r is the same as the impedance ratio (0.63). Considering that the wave speed of the sub-section S5 is 970 m/s, the wave speed in the anomaly is determined as 611 m/s. The determined wave speed is too high to fit into the typical range of wave speed for PVC water mains, which is typically from 300 to 500 m/s[40, 41]. As a result, the anomaly is unlikely to be a PVC pipe section with a length of 4 m.

The third possibility is that the anomaly is a small air pocket. The section of pipe between point PB and P23 is located in a hilly area with frequent elevation changes. As a result, small air pockets may be trapped at local high elevation points, although several air valves are used along the section. There are some noticeable pressure oscillations after the main reflection R5_B. In particular, after time t_b, the pressure rebounds from the lowest point and reaches a level much higher (approximately one third the size of the drop) than the pressure before the main drop (at time t_a). After that, a pressure drop much smaller than the main drop is seen and then the pressure recovers to the level before the main drop. The pressure oscillation after the main drop is a feature that has been seen in previous lab experiments on transient response of pipelines with small amount of trapped air [42]. The pressure oscillation after the main reflection as observed in the lab is believed to be introduced by the oscillation in the volume of the air pocket under transient event.

Summarising the previous analysis, it can be concluded that the anomaly corresponding to reflection R5_B in Figure 6 (or R5 in Figure 5) is most likely to be a small trapped air pocket in the pipeline. Other reflections (R1 to R4 and R6) can be analysed by the same procedure with the help of pressure traces measured at other locations. R1, R4 and R6 are induced by pipe class changes, R2 is likely to be a small air pocket and R3 is likely to be a PVC replaced section. The details of the analysis are not discussed here for brevity.

Conclusions

A field study has been conducted on non-invasive and non-destructive condition assessment for asbestos cement (AC) pipelines by time-domain fluid transient analysis. A sub-sectional condition assessment technique has been developed to determine the average wall condition of pipe sub-sections within a section bounded by two measurement points. Techniques previously used for detecting localised wall defects in metallic pipes have been further developed and adapted to AC pipes for the detection of significant localised anomalies to complement the sub-sectional condition assessment.

Field data collected from an AC water main with known pipe class changes has been used to verify the proposed techniques and illustrate the procedure of implementation. The pipe class changes have been successfully identified by the sub-sectional condition assessment. The wave speed, length and effective AC wall thickness of each sub-section have been determined, and the results are consistent with the values derived from the information given by the design drawings. The sub-sectional analysis also showed that the sub-sections under study have mild wall deterioration that is equivalent to uniform reduction in effective wall thickness of up to 2.3 mm. Because an AC pipe class change is essentially an AC wall thickness change, it is expected that the sub-sectional condition analysis can be also used for assessing extended wall deterioration in AC pipes with uniform class.

The procedure for localised defect detection in AC pipes using fluid transient waves has been illustrated. A localised anomaly located in the section of interest (between point PB and P23) has been identified and analysed in detail. The analysis showed that the anomaly is most likely to be a small air pocket.

This research, to the knowledge of the authors, is the first field verification of condition assessment of AC pipelines using fluid transient pressure waves. It has proved the concept that fluid transient pressure waves can be used as a tool for non-invasive and non-destructive condition assessment of AC pipelines, although the material properties and deterioration mechanisms are different from those of metallic pipelines. Compared to conventional selective sampling techniques[9], the proposed transient-based technique is non-destructive and covers much longer range; compared to the georadar technology[12], the proposed one is non-invasive and more efficient; and compared to the acoustic average wall thickness estimation technology[13], the proposed approach gives much more information about the pipe condition, including sub-sectional pipe condition and localised defects.

Acknowledgements

The research presented in this paper has been supported by the Australian Research Council through the Discovery Project Grant DP140100994. The authors thank East Gippsland Water (Victoria, Australia) and Victorian Water Industry Association for the support provided during the field testing.

References

1. Hu Y, Wang D, Cossitt K and Chowdhury R. AC pipe in North America: inventory, breakage, and working environments. *J Pipeline Syst Eng Prac*. 2010; 1: 156-72.
2. Al-Adeeb AM and Matti MA. Leaching corrosion of asbestos cement pipes. *Int J Cem Compos Lightweight Concrete*. 1984; 6: 233-40.
3. Matti MA and Al-Adeeb A. Sulphate attack on asbestos cement pipes. *Int J Cem Compos Lightweight Concrete*. 1985; 7: 169-76.
4. Wang D and Cullimore DR. Bacteriological challenges to asbestos cement water distribution pipelines. *J Environ Sci*. 2010; 22: 1203-8.

5. Wang D, Cullimore R, Hu Y and Chowdhury R. Biodeterioration of asbestos cement (AC) pipe in drinking water distribution systems. *Int Biodeter Biodegr*. 2011; 65: 810-7.
6. Gil L, Perez MA, Bernat E and Cruz JJ. Loss of strength in asbestos-cement water pipes due to leaching. *Struct Eng Mech*. 2011; 40: 655-63.
7. Hu Y, Wang D and Chowdhury R. Condition assessment methods for AC pipe and current practices. *Pipelines 2010: Climbing New Peaks to Infrastructure Reliability - Renew, Rehab, and Reinvest, August 28, 2010 - September 1, 2010*. Keystone, CO, United states: American Society of Civil Engineers, 2010, p. 867-77.
8. De Silva D, Davis P, Burn S, et al. Condition assessment of cast iron and asbestos cement pipes by in-pipe probes and selective sampling for estimation of remaining life. *20th International No-Dig Conference 2002*. Copenhagen, Denmark International Society for Trenchless Technology, 2002, p. Paper 2.1
9. Chowdhury R, Hu Y and Wang D. Condition evaluation of asbestos cement water mains. *Pipelines 2012: Innovations in Design, Construction, Operations, and Maintenance - Doing More with Less, August 19, 2012 - August 22, 2012*. Miami Beach, FL, United states: American Society of Civil Engineers (ASCE), 2012, p. 288-97.
10. Millette JR, Logsdon GS, Clark PJ and Kinman RN. Evaluating the condition of asbestos-cement pipe. *Mater Performance*. 1984; 23: 14-20.
11. Wang D, Hu Y and Chowdhury R. Examination of asbestos cement pipe deterioration with scanning electron microscopy. *Pipelines 2011: A Sound Conduit for Sharing Solutions, July 23, 2011 - July 27, 2011*. Seattle, WA, United states: American Society of Civil Engineers (ASCE), 2011, p. 65-78.
12. Smolders S, Verhoest L, De Gueldre G and Van De Steene B. Inspection of deteriorating asbestos cement force mains with georadar technique. *Water Sci Technol*. 2009; 60: 995-1001.
13. Bracken M, Johnston D and Coleman M. Acoustic based condition assessment of asbestos cement water transmission laterals. *Pipelines 2010: Climbing New Peaks to Infrastructure Reliability - Renew, Rehab, and Reinvest, August 28, 2010 - September 1, 2010*. Keystone, CO, United states: American Society of Civil Engineers, 2010, p. 815-25.
14. Beuken R, Horst P, Diemel R and Mesman G. Mains condition assessment by Echopulse, a validation of results. *Procedia Eng*. 2014; 89: 1437-44.
15. Ghidaoui MS, Zhao M, McInnis DA and Axworthy DH. A review of water hammer theory and practice. *Appl Mech Rev*. 2005; 58: 49-75.
16. Covas D, Ramos H and De Almeida AB. Standing wave difference method for leak detection in pipeline systems. *J Hydraulic Eng*. 2005; 131: 1106-16.
17. Lee PJ, Vítkovský JP, Lambert MF, Simpson AR and Liggett JA. Leak location using the pattern of the frequency response diagram in pipelines: a numerical study. *J Sound Vib*. 2005; 284: 1051–73.
18. Ferrante M, Brunone B and Meniconi S. Leak-edge detection. *J Hydraulic Res*. 2009; 47: 233-41.
19. Duan H-F, Lee PJ, Ghidaoui MS and Tung Y-K. Leak detection in complex series pipelines by using the system frequency response method. *J Hydraulic Res*. 2011; 49: 213-21.

517 20. Ghazali MF, Staszewski WWJ, Shucksmith JD, Boxall JB and Beck SBM. Instantaneous
518 phase and frequency for the detection of leaks and features in a pipeline system. *Struct Health*
519 *Monit*. 2011; 10: 351-60.
520 21. Gong J, Lambert MF, Simpson AR and Zecchin AC. Single-event leak detection in pipeline
521 using first three resonant responses. *J Hydraulic Eng*. 2013; 139: 645-55.
522 22. Wang XJ, Lambert MF and Simpson AR. Detection and location of a partial blockage in a
523 pipeline using damping of fluid transients. *J Water Resour Plan Manage*. 2005; 131: 244-9.
524 23. Sattar AM, Chaudhry MH and Kassem AA. Partial blockage detection in pipelines by
525 frequency response method. *J Hydraulic Eng*. 2008; 134: 76-89.
526 24. Duan H-F, Lee PJ, Ghidaoui MS and Tung Y-K. Extended blockage detection in pipelines
527 by using the system frequency response analysis. *J Water Resour Plan Manage*. 2012; 138: 55-
528 62.
529 25. Meniconi S, Duan HF, Lee PJ, Brunone B, Ghidaoui MS and Ferrante M. Experimental
530 investigation of coupled frequency and time-domain transient test-based techniques for partial
531 blockage detection in pipelines. *J Hydraulic Eng*. 2013; 139: 1033-44.
532 26. Meniconi S, Brunone B and Ferrante M. In-line pipe device checking by short-period
533 analysis of transient tests. *J Hydraulic Eng*. 2011; 137: 713-22.
534 27. Hachem FE and Schleiss AJ. Detection of local wall stiffness drop in steel-lined pressure
535 tunnels and shafts of hydroelectric power plants using steep pressure wave excitation and
536 wavelet decomposition. *J Hydraulic Eng*. 2012; 138: 35-45.
537 28. Stephens ML, Lambert MF and Simpson AR. Determining the internal wall condition of
538 a water pipeline in the field using an inverse transient model. *J Hydraulic Eng*. 2013; 139: 310–
539 24.
540 29. Gong J, Simpson AR, Lambert MF, Zecchin AC, Kim Y and Tijsseling AS. Detection of
541 distributed deterioration in single pipes using transient reflections. *J Pipeline Syst Eng Prac*. 2013;
542 4: 32-40.
543 30. Gong J, Stephens ML, Arbon NS, Zecchin AC, Lambert MF and Simpson AR. On-site non-
544 invasive condition assessment for cement mortar-lined metallic pipelines by time-domain fluid
545 transient analysis. *Struct Health Monit*. 2015; 14: 426-38.
546 31. Lee PJ, Duan HF, Ghidaoui M and Karney B. Frequency domain analysis of pipe fluid
547 transient behaviour. *J Hydraulic Res*. 2013; 51: 609-22.
548 32. Covas D, Stoianov I, Mano JF, Ramos H, Graham N and Maksimovic C. The dynamic effect
549 of pipe-wall viscoelasticity in hydraulic transients. Part I - Experimental analysis and creep
550 characterization. *J Hydraulic Res*. 2004; 42: 516-30.
551 33. Duan H-F, Lee PJ, Ghidaoui MS and Tung Y-K. System response function-based leak
552 detection in viscoelastic pipelines. *J Hydraulic Eng*. 2012; 138: 143-53.
553 34. Meniconi S, Brunone B, Ferrante M and Massari C. Energy dissipation and pressure
554 decay during transients in viscoelastic pipes with an in-line valve. *J Fluids Struct*. 2014; 45: 235-
555 49.

35. Stephens ML. *Transient response analysis for fault detection and pipeline wall condition assessment in field water transmission and distribution pipelines and networks,* PhD Thesis, University of Adelaide, Adelaide, Australia, 2008.
36. Chaudhry MH. *Applied Hydraulic Transients*. 3rd ed. New York, NY: Springer, 2014.
37. Wylie EB and Streeter VL. *Fluid Transients in Systems*. Englewood Cliffs, New Jersey, USA: Prentice Hall Inc., 1993, p.463.
38. Gong J, Lambert MF, Simpson AR and Zecchin AC. Distributed deterioration detection in single pipes using the impulse response function. *14th International Conference on Water Distribution Systems Analysis (WDSA 2012)*. Adelaide, South Australia: Engineers Australia, 2012, p. 702-19.
39. Standards Australia. *Australian standard specification - Asbestos cement pressure pipes* (AS 1711-1975). Sydney, NSW, Australia: Standards Australia, 1975.
40. Watters GZ, Jeppson RW and Flammer GH. Water hammer in PVC and reinforced plastic pipe. *J Hydr Eng Div*. 1976; 102: 831-43.
41. Seipt WR. Waterhammer considerations for PVC pipeline in irrigation systems. *T ASAE*. 1974; 17: 417-23.
42. Kim Y. *Advanced Numerical and Experimental Transient Modelling of Water and Gas Pipeline Flows Incorporating Distributed and Local Effects,* PhD thesis, University of Adelaide, Adelaide, 2008.

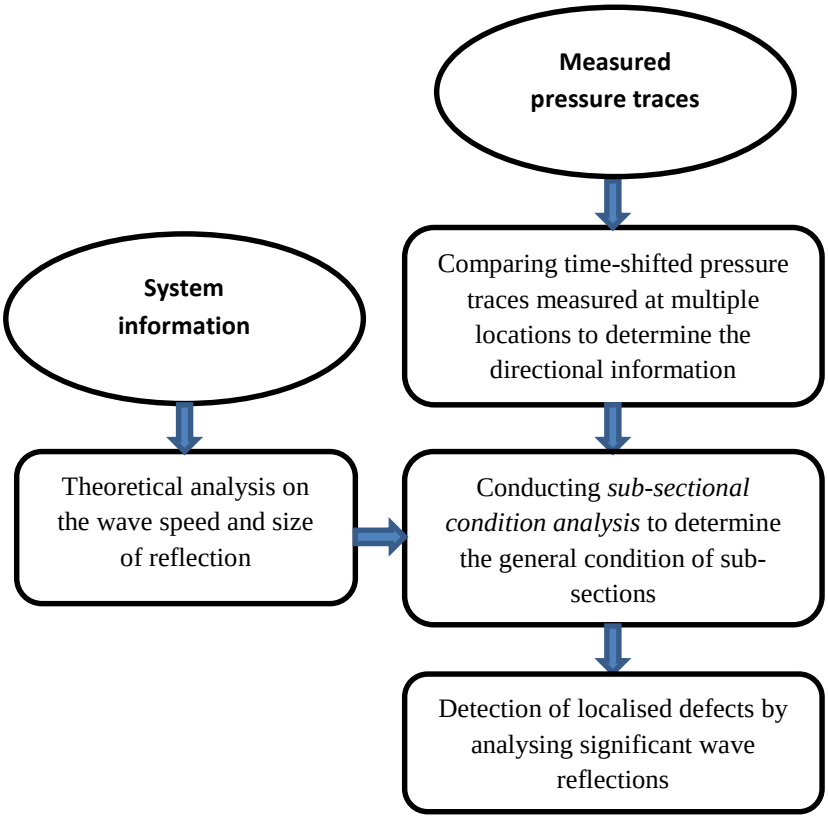

Figure 1. Flowchart illustrating the procedure of data analysis for transient-based pipeline condition assessment.

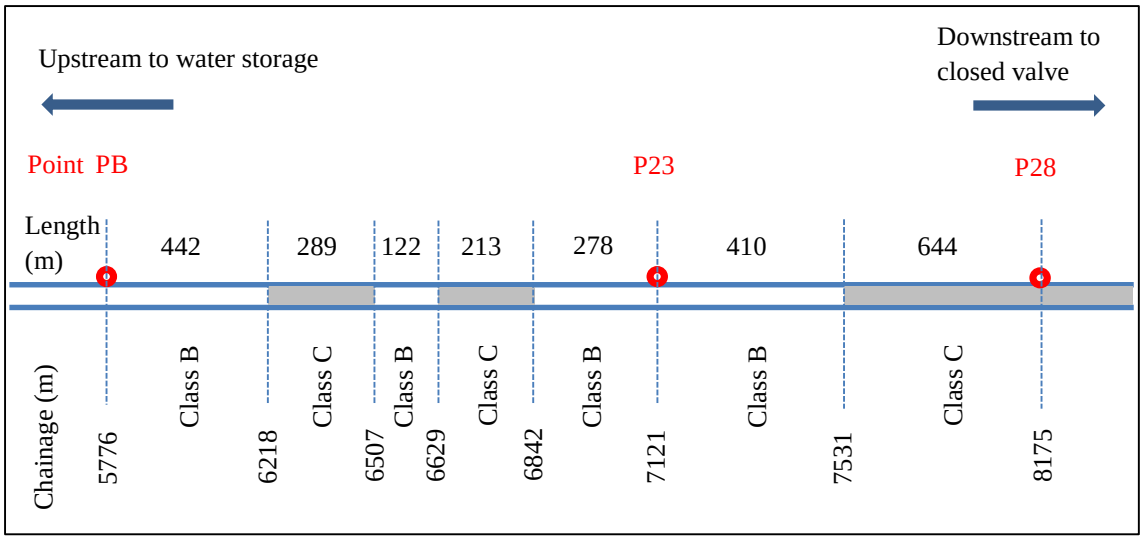

Figure 2. Layout of the section of AC pipeline under test as given by the design drawings [white sections represent Class B (nominal wall thickness 17.3 mm) and grey sections are Class C (nominal wall thickness 25.4 mm)].

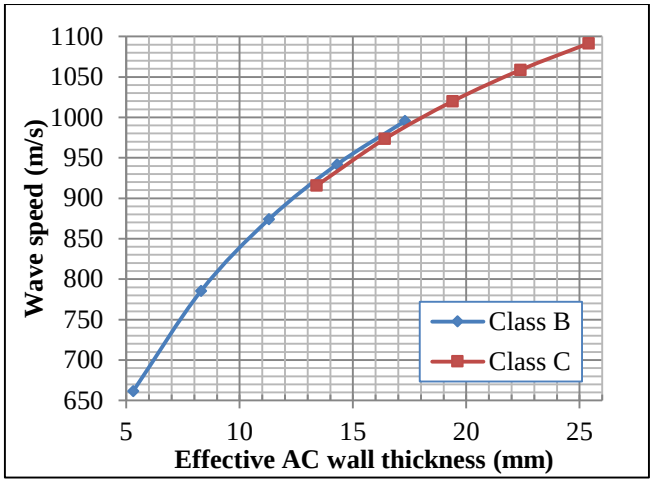

Figure 3. Theoretical wave speeds for DN300 AC pipeline (Class B and C) with varying effective AC wall thickness (the right end of each line represents the original intact condition).

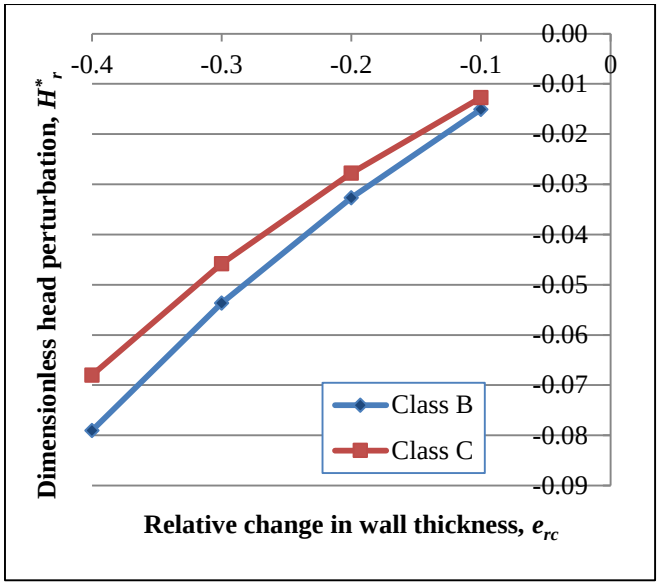

Figure 4. Variation in the dimensionless head perturbation (H_r^*) according to various relative change in wall thickness (e_{rc}) for both Class B and Class C AC pipes.

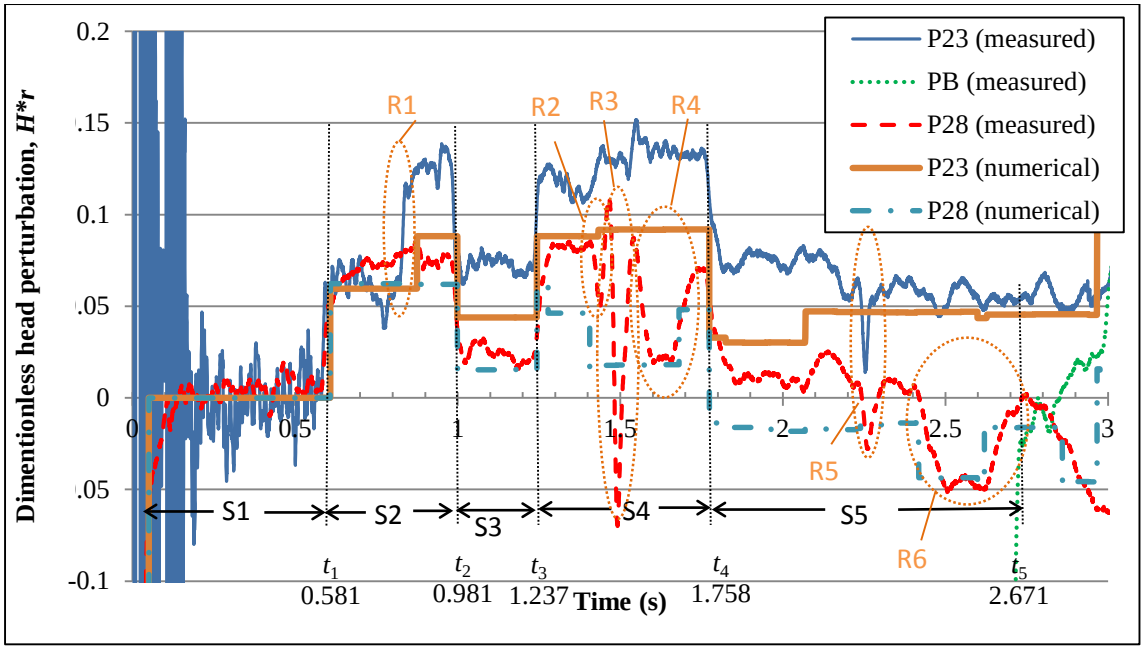

Figure 5. Dimensionless head perturbations measured at points P23 (thin solid line), PB (dotted line) and P28 (dashed line) with generation at P23, and corresponding numerical dimensionless head perturbations at points P23 (thick solid line) and PB (dash-dotted line) according to the change in pipe classes shown in the design drawings. The traces are time-shifted to line up reflections coming from the upstream side (the direction towards PB) of P23. S1 to S5 represents five sub-sections for analysis between PB and P23, R1 to R6 are significant reflections for localised defect detection.

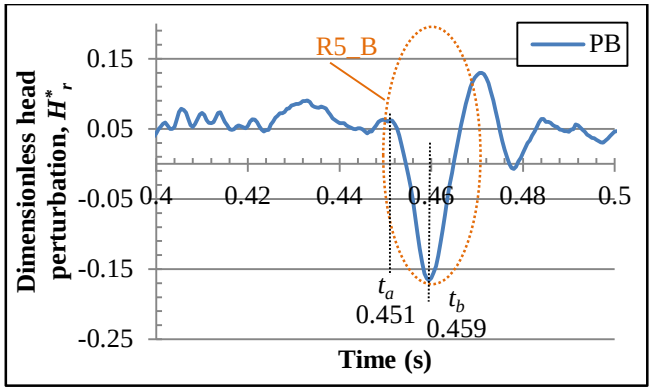

Figure 6. Dimensionless head perturbations measured at point PB with generation at PB. Reflection R5_B is induced by the anomaly that corresponds to R5 in the test shown in Figure 5.

Table 1. Physical properties of Class B and Class C DN300 AC pipe at a water temperature of 25 ºC.

Physical Properties at 25ºC	**300 AC Class B**	**300 AC Class C**
Outside diameter (OD)	333.8 mm	345.4 mm
Inside diameter (ID)	299.2 mm	294.6 mm
Wall thickness (e_0)	17.3 mm	25.4 mm
Modulus of elasticity (E_C)	32 GPa	32 GPa
Bulk modulus of water (K)	2.24 GPa	2.24 GPa
Density of water (ρ)	997.1 kg/m^3	997.1 kg/m^3
Poisson's ratio (μ)	0.2	0.2
Constraint factor (c)	1.05	1.09
Theoretical wave speed	996 m/s	1092 m/s
Design pressure	1.2 MPa	1.8 MPa

Table 2. Determined wave speeds, lengths and effective AC wall thicknesses for the five sub-sections between PB and P23, with comparison to the theoretical values for intact pipes.

Sub-section	Wave speed (m/s)		Length (m)		Effective wall thickness (mm)	
	Theoretical	Determined	From drawings	Determined	Theoretical	Determined
S1	996	976	278	284	17.3	16.2
S2	1092	1076	213	215	25.4	24
S3	996	982	122	126	17.3	16.5
S4	1092	1066	289	278	25.4	23.1
S5	996	970	442	443	17.3	15.8